ICSO 2016

International Conference on Space Optics

Biarritz, France

18–21 October 2016

Grism manufacturing by low temperature mineral bonding

G. Kalkowski

K. Grabowski

G. Harnisch

T. Flügel-Paul

et al.

GRISM MANUFACTURING BY LOW TEMPERATURE MINERAL BONDING

G. Kalkowski, K. Grabowski, G. Harnisch, T. Flügel-Paul, U. Zeitner, and S. Risse
Fraunhofer Institut für Angewandte Optik und Feinmechanik, 07745 Jena, Germany

INTRODUCTION

By uniting a grating with a prism to a GRISM compound, the optical characteristics of diffractive and refractive elements can be favorably combined to achieve outstanding spectral resolution features. Ruling the grating structure into the prism surface is common for wavelengths around 1 µm and beyond, while adhesive bonding of two separate parts is generally used for shorter wavelengths and finer structures. We report on a manufacturing approach for joining the corresponding glass elements by the technology of hydrophilic direct bonding. This allows to manufacture the individual parts separately and subsequently combine them quasi-monolithically by generating stiff and durable bonds of vanishing thickness, high strength and excellent transmission. With this approach for GRISM bonding, standard direct-write- or mask-lithography equipment may be used for the fabrication of the grating structure and the drawbacks of adhesive bonding (thermal mismatch, creep, aging) are avoided.

The technology of hydrophilic bonding originates from "classical" optical contacting [1], but has been much improved and perfected during the last decades in the context of 3-dimensinal stacking Si-wafers for micro-electronic applications [2]. It provides joins through covalent bonds of the Si-O-Si type at the nanometer scale, i.e. the elementary bond type in many minerals and glasses. The mineral nature of the bond is perfectly adapted to most optical materials and the extremely thin bonding layers generated with this technology are well suited for transmission optics. Creeping under mechanical load, as commonly observed with adhesive bonding, is not an issue. With respect to diffusion bonding, which operates at rather high temperatures close to the glass transition or crystal melting point, hydrophilic bonding is a low temperature process that needs only moderate heating. This facilitates provision of handling and alignment means for the individual parts during the set-up stages and greatly eases joining optical materials of different thermal expansion.

The technology has been successfully used in the past for bonding various glasses as well as crystalline optical materials [3, 4]. Here we will focus on bonding prisms elements and binary gratings of fused silica with and without coatings at the bonding interface. Further, preliminary results on bonding prism-grating-prism (PGP) combinations will be presented.

BONDING PRINCIPLE

Hydrophilic direct bonding requires smooth and plane (or highly conformal) glass surfaces. An extremely low surface roughness on the spacial frequency scale of atomic-force microscopy (AFM) is mandatory. Although bonding becomes possible at an AFM roughness of about 1 nm root-mean-square (RMS), values of <0.3 nm RMS are recommended to obtain high bond strength. For thick and stiff specimen –like prisms– about $\lambda/10$ flatness peak-to-valley (PV) is required ($\lambda= 633$ nm), while this requisite may be relaxed by more than an order of magnitude for thin and flexible substrates. The latter applies to glass wafers or mask blanks up to thickness ≈1/8 inch according to our experience.

Bonding works without specific additives after careful wet cleaning and low pressure plasma activation for generating "super-hydrophilic" surface conditions at the bonding interfaces. Through sophisticated surface preparation, favorable conditions for sticking OH groups from adsorbed water molecules to both surfaces are generated. In standard Si-wafer bonding, full manual contact of both parts is mediated under vacuum and subsequent bonding proceeds by applying hydraulic pressure of the order of 1 MPa on both parts to achieve intimate surface contact. The change-over from temporary weak Van-der-Waals bonding to permanent strong covalent bonding takes place at temperatures of about 200…300°C through a condensation reaction of opposing OH groups on the two surfaces with the subsequent release of water. The basic reaction is schematically described by the equation

$$X–Si–OH \; + \; OH–Si–X \; \rightarrow \; X–Si–O–Si–X \; + H2O \uparrow \tag{1}$$

Here X stands for the bulk environment of a Si atom in the top layer of the glass surfaces. Oxygen "bridges", i.e. covalent oxygen bonds are formed between the neighboring glass surfaces and provide the final "glue" for connecting both parts. The water emerging from the condensation reaction is driven out of the bonding zone by diffusion into interstitial voids or the surrounding vacuum environment during the final heat treatment.

PROCESS OF GRISM BONDING

Aside from ambitious flatness and roughness requirements on the surfaces of the two bonding partners, cleanliness of the bonding interfaces from particles is important and requires careful preparation in a clean room environment. In our GRISM manufacturing approach, cleaning, plasma activation and contacting proceed in a ISO class 3 clean room environment. Except for contacting, the process sequence is the same as previously described for joining fused silica glass wafers [5]. However, while the latter are transferred into a vacuum device before full area contacting and bonding, this is currently not possible with GRISM manufacturing, due to the bulky nature of the prisms and the single-part production conditions. Instead, individually designed equipment for the respective GRSIM dimensions has to be allocated, and mounting as well as contacting of both parts proceeds at ambient conditions. Accurate alignment of the dispersion plane of the grating to the prism angle is important and requires sophisticated adaptation of the bond equipment to specific reference areas of both parts during the production flow.

The design of a typical GRISM bonding device is schematically illustrated in Fig. 1. Basically, a V-groove holder supports the prism kinematically from below and allows for an easy access to the joining area at the top. The grating is placed from above onto the bonding surface of the prism, aligned and mechanically fixed. In the set-up of Fig. 1, one of the triangular sides of the prism –which are polished, flat and sufficiently parallel to the prism angle– was chosen as reference area for the alignment process. For the grating element, the mechanical edge on one of its long sides was carefully prepared for alignment. This can be achieved by applying a highly precise cut when the grating is separated from the mask blank after lithographic exposure and structuring. Depending on its length, the edge can be cut to about 10 arcsec precision in parallel to alignment marks that represent the grating orientation with lithographic accuracy. Finally, a flat jig (at the back side of the device in Fig. 1) can be used as mechanical stop for passive alignment of both parts.
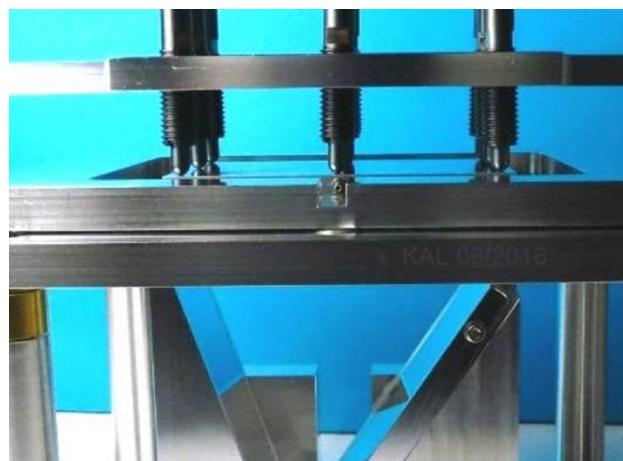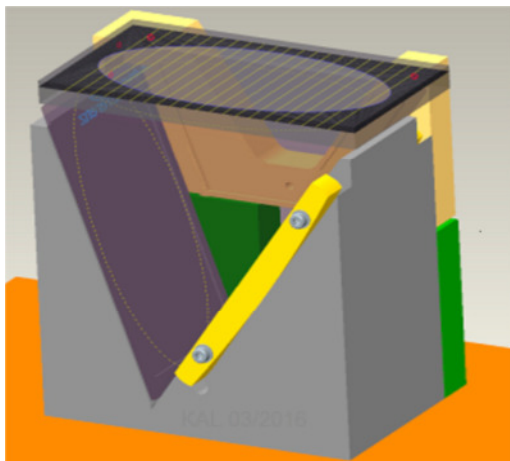

Fig. 1. GRISM bonding device (scheme)   **Fig. 2.** Compressing both parts during heat treatment

With proper contacting provisions, the top part initially "swims" on an air-cushion before settling down on the bottom part under ambient conditions. This period can be used for alignment. After touch-down, the orientation is slightly friction-locked and can be durably fixed by compressive spring elements –as seen in Fig. 2– or other compressing means for the adjacent heat treatment under vacuum (or protective gas atmosphere). Heating starts immediately afterwards and may extend from about 8 h to more than 48 h, depending on the heat capacities involved and the selected temperature profiles. If 200°C is chosen as maximal temperature for bonding fused silica, this temperature level should be maintained for at least 4 h to achieve high bond strength, according to our experience.

EXAMPLES OF GRISM BONDING

As illustrated below, various GRISM configurations were manufactured from fused silica components by direct bonding at temperatures of ≈200°C in vacuum. Initially, binary gratings were generated on 5009 type mask blanks of thickness 2.3 mm and cut to lateral dimensions of 55x55 mm². Fig. 3 shows the result of bonding the unstructured backside of such a grating to a prism element. To protect the grating structure from damage during

the handling period and the heat treatment under compression, a protective glass cover was temporarily applied to the grating surface by adhesive bonding.
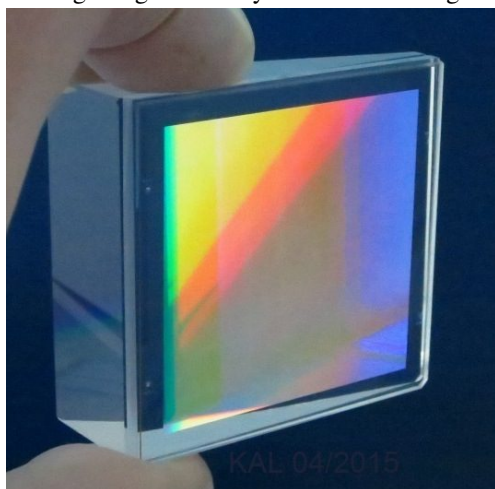

Fig. 3. GRISM bond with (uncoated) grating at the outer surface
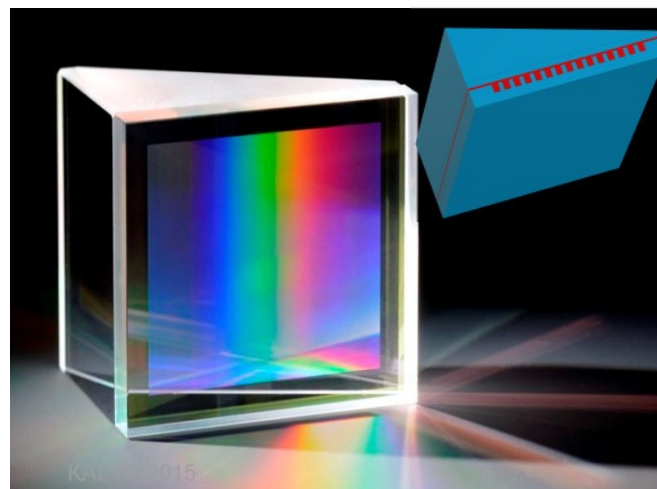

Fig. 4. GRISM bond with (coated) grating at the inside (compare scheme at top right)

Figure 4 shows the result of bonding a square grating of approx. size 50x50x6.3 mm³ to a right angle prism. In this case, the grating area is located at the bonding interface as schematically indicated at the top right. It comprises a binary structure of period 441 nm and approximate area 40x40 mm² generated from a 6025 type mask blank. Before bonding, the grating was completely filled with high index material by atomic layer deposition (ALD) and covered with a top layer of SiO_2 for chemical adaptation to the prism.

Similar bonds as in Fig. 3 –with an unfilled grating at the outside– were performed with gratings of size 120x65x6.3 mm³ to approximately equilateral triangular prisms of 65 mm height. Figure 5 displays a typical bonding result. Again, the structured surface was temporarily protected by a cover-glass during the bonding process. The basic set-up for manufacturing this relatively large GRISM element is schematically illustrated in Fig. 1 above and the strategy and results of gating alignment are outlined below.

Our current development activities focus on manufacturing prism-grating-prism (PGP) compounds by this technology. Figure 6 shows preliminary results of successful bonding plane-parallel prism-dummies from both sides to a binary grating element. Square shaped glass blanks of lateral size 55x55 mm² and thickness 20 mm were used to roughly simulate the stiffness of future prism elements. The grating element at the center is 3.2 mm thick but otherwise of similar structure as in Fig. 3 above, i.e. a binary grating with an unstructured rim of about 5 mm width to enhance adhesion on this side. Bonding proceeds in two successive steps, with the grating side bonded first –since it represents less bonding area– to take advantage of the grating flexibility at this stage.
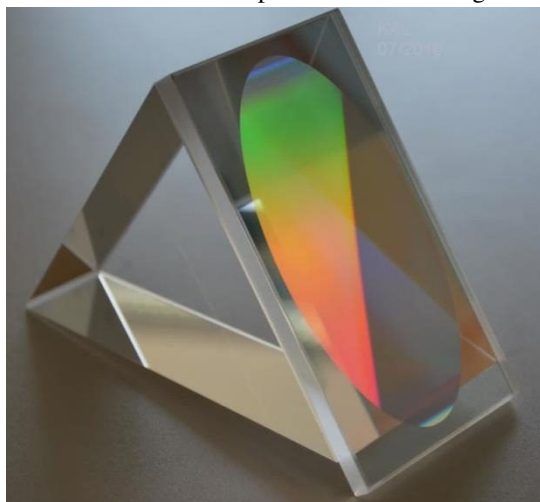

Fig. 5. GRISM bond with ALD-coated grating at the outer surface

Fig. 6. Prism-grating-prism type bond using prism dummies of plane-parallel shape

Before executing the second bond, the backside of the grating is inspected and eventually reworked with respect to flatness and roughness to provide optimal bonding conditions. In general, the second bonding step is more demanding than the first and requires flatness improvement, since stiffness of both bonding partners is quite high and thickness variations of the mask blank add up to the flatness deviations at the first bonding interface. Also, compression is slightly increased relative to the first bond, in general, since intimate contact between both surfaces harder to achieve, but necessary for successful bonding,

CHARACTERIZATION OF GRISM BONDS

A. Bond strength (Static)

Bond strength testing proceeds by destructive 3-point bending tests on beam-like specimen, that are cut out of the bonded compound with a diamond saw. Figure 7 illustrates the approach for the PGP-testbond in Fig. 6. Specimen of approx. dimension 43x9.5x9.5 mm³ were prepared. A Zwick-Roell testing machine (type Z020 Alround-line) and a 3-point bending testing set-up as illustrated in the figure are used routinely in our lab to test ensembles of about 10 specimen. In view of the grating induced anisotropy, the direction of load impact is chosen in parallel to the groove run, when a structured grating side is involved in bonding. This orientation represents the direction of least bond strength [5, 6], due to the reduced contact area that is provided by only the ridges of the binary grating.

In the exemplary PGP-testbond, ridge width amounts to about 1/3 of the grating period and breakage occurred neatly at the structured side of the grating element in nearly all cases. To the right of Fig. 7, a Weibull analysis of the measured bond strength values is shown, indicating a value of about 13 MPa for the 63% characteristic stress at breakage. When extrapolated to full area contact by multiplication with a factor 3, this would amount to about 39 MPa, i.e. about 40% of the bond strength determined for massive fused silica bulk material. Compared to previously determined bond strengths of ≥70 MPa for joining unstructured fused silica blanks of optimal surface quality, the current value may still bear potential for improvement.
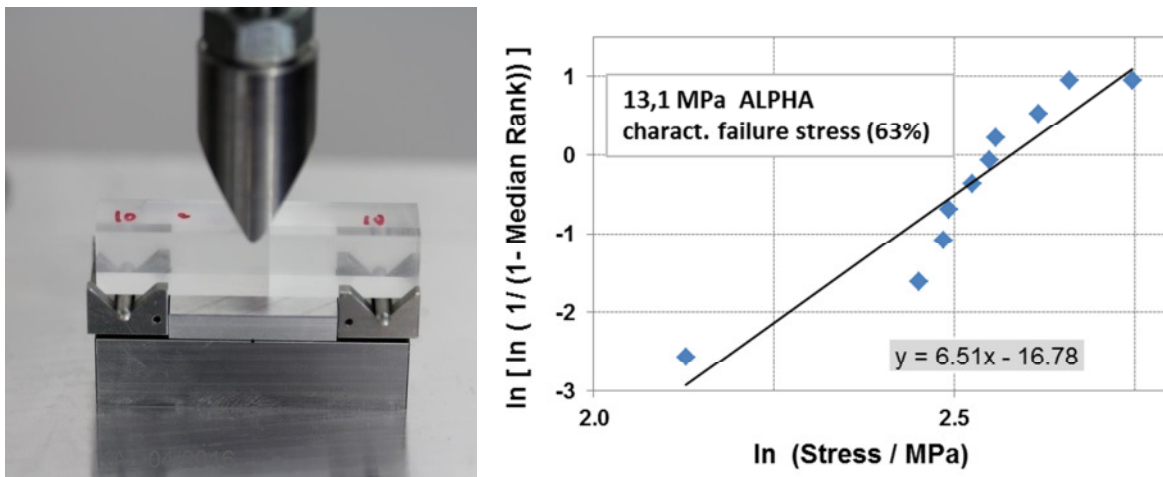

Fig. 7. Set-up for 3-point bending test (left) and Weibull analysis of bond strength values (right)

B. Bond strength (Dynamic)

In addition to static tests, shock and vibration tests are performed occasionally. Figure 8 displays the set-up and results for shock testing a specimen in a preliminary stage of GRISM-bonding. The specimen is related to the configuration if Fig. 3 (grating outside) and tests were performed with respect to all three orthogonal directions of a Cartesian coordinate system at a certified institution. As visible to the left in Fig. 8, acceleration sensors are connected to the specimen as well as the mounting frame during these tests. To the right of Fig. 8, the constraints for shock testing along the normal of the bonding interface (z-axis) are detailed. The horizontal axis spans the frequency range of 100 to 10000 Hz and the the vertical axis indicates acceleration (in units of earth

gravity (g)). No defects were discernable after completion of all tests, indicating that bond stability is sufficient at this stage for the usual requirements on optical equipment to survive a rocket start.
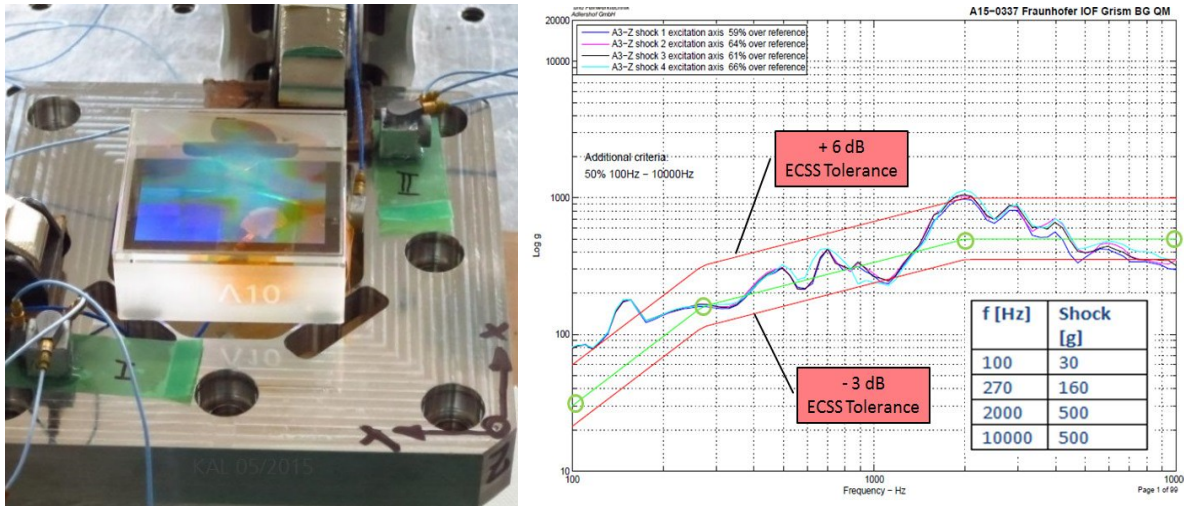

Fig. 8. Set-up for shock test (left) and corresponding z-axis acceleration vs. frequency diagram (right)

C. Alignment

Grating alignment can be measured by tactile as well as optical means in our lab. In the tactile approach, a 3d coordinate measuring machine with an optical sensor for detection of the alignment marks on the grating side is used. In the optical approach, a calibrated device –consisting of a rotary table equipped with an angle encoder in combination with an electronic auto-collimator– is utilized. As is shown to the left in Fig. 9, this set-up was applied to characterize the grating alignment for GRISM bonds of the type of Fig. 5.

After calibrating the horizontal line induced by the rotary table, the directions of the normals to the prism surfaces are evaluated from the auto-collimator and angle measurements. Subsequently, the orientations of the relevant prism edges are calculated from the corresponding vector products. Finally, the grating orientation is determined from measuring the back reflections in the -1st and +1st diffraction order.

The angles between the dispersion direction of the grating and two of the three prism edges as determined from four consecutive measurements are shown in the table to the right of Fig. 9. As can be seen, a quite high precision and reproducibility of the data was achieved and deviations from perfect alignment (90°) amount to less than 1 arc min. This value is considered trustful, although accuracy of the measurements still needs to be verified by comparison to the tactile approach or corresponding measurements at a certified institution.
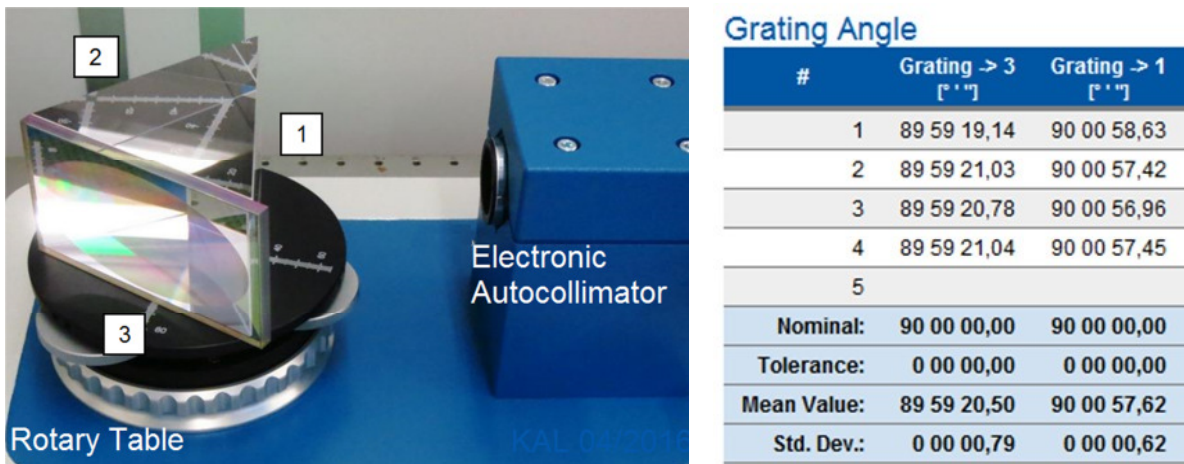

Grating Angle		
#	Grating -> 3 [° ' "]	Grating -> 1 [° ' "]
1	89 59 19,14	90 00 58,63
2	89 59 21,03	90 00 57,42
3	89 59 20,78	90 00 56,96
4	89 59 21,04	90 00 57,45
5		
Nominal:	90 00 00,00	90 00 00,00
Tolerance:	0 00 00,00	0 00 00,00
Mean Value:	89 59 20,50	90 00 57,62
Std. Dev.:	0 00 00,79	0 00 00,62

Fig. 9. Set-up for alignment test (left) and results of angular orientation of grating vs. prism edges (right)

SUMMARY AND OUTLOOK

The technology of hydrophilic direct bonding has been outlined and applied to generate GRISM compounds from fused silica elements. Plane parallel prism dummies of lateral size 55x55 mm² and thickness 20 mm, right angle prisms of similar size and even larger triangular prisms of approximate edge length 120 mm and height 65 mm were successfully bonded to the corresponding binary grating elements. The latter were generated from fused silica mask blanks of 5009, 6025 and 6012 type by e-beam lithography and dry etching. Both sides of the gratings, i.e. the structured as well as the unstructured sides, could be reliably joined to the corresponding prism partners. Even the ALD filled grating side proved to be bondable after suitable surface preparation.

Bond strength depends on flatness and roughness conditions at the corresponding surfaces. Bonding the structured grating side of a binary grating with a ridge-to-groove width ratio of about 1:2 to a plane surface resulted in a static bond strength of about 13 MPa, which corresponds to about 39 MPa, when normalized to the effective bond area provided by the ridges only. This value is about 30 MPa less than previously measured for unstructured fused silica blanks of optimal surface quality, but should be sufficient for most applications.

Further, alignment strategy and alignment measurements for GRISM direct bonding were presented. With a dedicated bonding device and passive alignment means, a large grating of about 120 mm length could be bonded with about 1 arcmin accuracy relative to the prism angles, according to preliminary optical measurements.

We conclude, that direct bonding is a new joining technology for future GRISM manufacturing that may be well suited for extremely demanding applications as encountered in space.

Future work aims at manufacturing prism-grating-prism compounds with this technology. Preliminary results were presented and appear quite promising.

ACKNOWLEDGEMENT

REFERENCES

[1] J. Haisma, B. Spierings, U. Biermann, and A. van Gorkum, "Diversity and feasibility of direct bonding: A survey of a dedicated optical technology", Applied Optics, Vol. 33 (7) 1154-1169 (1994).
[2] Q.-Y. Tong, U. Gösele, *Semiconductor Wafer Bonding*, John Wiley & Sons, New York (1999).
[3] G. Kalkowski, S. Risse, U. Zeitner, F. Fuchs, R. Eberhardt, A. Tünnermann, "Glass-Glass Direct Bonding", ECS Transactions, Vol. 64 (5) 3-11 (2014).
[4] C. Rothhardt, M. Rekas, G. Kalkowski, N. Haarlammert, R. Eberhardt, and A. Tünnermann, "Fabrication of a high power Faraday isolator by direct bonding", Proc. of SPIE, Vol. 8601 (2013) 86010T-1.
[5] G. Kalkowski, U. Zeitner, T. Benkenstein, J. Fuchs, C. Rothhardt, and R. Eberhardt, "Direct wafer bonding for encapsulation of fused silica optical gratings", Microelectronic Engineering 97, 177-180 (2012).
[6] Ö. Vallin, K. Jonsson, U. Lindberg, "Adhesion quantification methods for wafer bonding", Mat. Science and Engineering R 50, 109–165 (2005).